Journal of Applied Polymer Science

Antibacterial Activity and Cytotoxicity of Hydrogel–Nanosilver Composites Based on Copolymers from 2-Acrylamido-2-methylpropanesulfonate Sodium

Hernán Valle,[1] Bernabé L. Rivas,[1] Mar Fernández,[2] María A. Mondaca,[3] María R. Aguilar,[2] Julio San Román[2]

[1]Polymer Department, Faculty of Chemistry, University of Concepción, Casilla 160-C, 4089100 Concepción, Chile
[2]Biomaterials Department, Institute of Polymer Science and Technology, Consejo Superior de Investigaciones Científicas (CSIC), Juan de la Cierva 3, 28006 Madrid, Spain
[3]Microbiology Department, Faculty of Biological Sciences, University of Concepción, Casilla 160-C, 4089100 Concepción, Chile
Correspondence to: B. L. Rivas (E-mail: brivas@udec.cl)

ABSTRACT: In this research, we contributed to the search for potential hydrogel–silver dressings by generating hydrogel–silver nanoparticles (AgNPs) composites prepared by the dipping of the crosslinked hydrogel poly(*N*-vinylpyrrolidone-*co*-2-acrylamido-2-methylpropanesulfonate sodium) (1:1) and poly(acrylamide-*co*-2-acrylamido-2-methylpropanesulfonate sodium) (1:1) into an aqueous suspension of citrate-stabilized AgNPs. The composites obtained were evaluated by an antibacterial activity assay on *Staphylococcus aureus* and *Escherichia coli* and subjected to an *in vitro* cytotoxicity assay for human fibroblasts. The composite formed from the hydrogel poly(*N*-vinylpyrrolidone-*co*-2-acrylamido-2-methylpropanesulfonate sodium) with 3 mol % *N*,*N*-methylene bisacrylamide showed the highest antibacterial activity and the least cytotoxicity among the composites tested; this makes it an excellent alternative as a potential dressing for the treatment of deep and exudative wounds. © 2013 Wiley Periodicals, Inc. J. Appl. Polym. Sci. **2014**, *131*, 39644.

KEYWORDS: composites; copolymers; nanoparticles; nanowires and nanocrystals

Received 30 March 2013; accepted 10 June 2013
DOI: 10.1002/app.39644

INTRODUCTION

Bacterial infections remain a major cause of morbidity in patients with burns and skin wounds and are thus a public health problem worldwide.[1] A growing trend in the treatment of these infections is the use of hydrogel dressings that release silver nanoparticles (AgNPs), which have excellent antibacterial activity on a broad spectrum of Gram-negative and Gram-positive bacteria. It has been demonstrated that AgNPs smaller than 10 nm are basically responsible for the antibacterial action.[2] Furthermore, the hydrogel absorbs wound exudate, maintains a moist environment, enables the sustained release of the AgNPs, and prevents the need for frequent replacement, which is necessary with other fabric-based dressings.[3]

The mechanism for the antimicrobial activity of the AgNPs is not fully understood. The three most common mechanisms proposed are (1) the gradual release of free silver ions followed by the disruption of ATP production and DNA replication, (2) the AgNPs direct damage to cell membranes, and (3) the AgNPs and silver ion generation of reactive oxygen species.[4]

In comparison to bacterial cells, human cells are less sensitive to the toxic effect of AgNPs (and the silver ions) because human cells have a greater structural and functional complexity. The previous statement can be illustrated by consideration of the structural differences of the electron transfer chain (ETC) among bacterial and human cells. The bacterial ETC is located in the cell envelope (cell exterior), whereas the ETC of human cells are found intracellularly in the mitochondrial organelles, and therefore, the silver ions (or AgNPs) have easier access to the bacterial ETC to inactivate it. For comparable inactivation of mitochondrial ETC proteins, higher silver concentrations are required because the cellular membrane acts as a diffusion barrier and must be overcome first. Moreover, in contrast to the single ETC of each bacterial cell, each human cell generally has several mitochondria, which allows it to continue producing biological energy, even when some of them have been inactivated for silver ions or AgNPs.[5]

Despite the important advances in the field of hydrogel–silver dressings, the main challenge remains optimization of the

balance between antibacterial efficacy and cytotoxicity. Therefore, various new methods and materials are currently being investigated.[6,7] Although there are currently several hydrogel–AgNPs dressings commercially available for use, the results of several studies of their antibacterial efficacy and cytotoxicity have been contradictory.[6,8]

The various degrees of cytotoxicity (in human cells) and antibacterial activity of these dressings are related directly to the amount of total silver incorporated into and released from their polymeric matrix (hydrogel),[3] which in turn depends on the chemical nature of the pendant groups of the copolymer main chain and its degree of crosslinking.[7] For this reason, the search for more efficient hydrogel–AgNPs dressings has continued in recent years, with particular focus on obtaining a polymer matrix that allows the controlled release of AgNPs.

Polymers containing 2-acrylamido-2-methylpropanesulfonate sodium (AMPSNa) monomer have a high water-absorbing capacity (it is pH-independent) and electrical conductivity because of its strongly ionizable sulfonate group; this makes them ideally suited for applications such as wound care dressings, drug delivery, transdermal patches, and electrocardiograph electrodes. Other polymer properties enhanced by AMPSNa are thermal stability, resistance to hydrolysis, softness, flexibility, transparency, and facility to remove any residual unreacted monomer by water when the polymerization is performed in an aqueous system.[9,10]

Equally important are the medical applications of *N*-vinylpyrrolidone (VP)-based copolymers and acrylamide (AAm)-based copolymers. The VP-based copolymers are used as plasma substitutes, water-soluble drug carriers, and UV-curable bioadhesives because of its good biocompatibility, low toxicity, good film formation, and adhesive characteristics; these properties are associated with the amphiphilic characteristics of the VP monomer because it contains a highly polar amide group (which is hydrophilic) along with apolar methylene and methine groups (hydrophobic) in the backbone and the ring.[11–13] On the other hand, AAm-based copolymers are used as soft-tissue implants, supports for enzyme and cell immobilization, hydrogels for controlled drug release and other uses[14–16] because they exhibit a high water absorption capability, permeability to oxygen and possess good biocompatibility.[14]

The aforementioned background gave rise to this investigation, in which four hydrogel–AgNPs composites based on copolymers of AMPSNa with VP and AAm, were obtained by an *ex situ* method, subsequently assessed with an antibacterial activity assay against *Staphylococcus aureus* and *Escherichia coli,* and subjected to an *in vitro* cytotoxicity assay on human fibroblasts.

The synthesized hydrogels were poly(*N*-vinylpyrrolidone-*co*-2-acrylamido-2-methylpropanesulfonate sodium) [poly(VP-*co*-AMPSNa), 1:1], which has not been previously reported as a support for AgNPs, and poly(acrylamide-*co*-2-acrylamido-2-methylpropanesulfonate sodium) [poly(AAm-*co*-AMPSNa), 1:1]. In the preparation of the four hydrogels, 3 and 6 mol % *N,N*-methylene bisacrylamide (MBA; crosslinking reagent) were used. The AgNPs obtained by the chemical reduction of aqueous silver nitrate ($AgNO_3$) and stabilized with sodium citrate were incorporated into the hydrogels by immersion of the xerogel into the colloidal dispersion of AgNPs.

EXPERIMENTAL

Materials

AMPSNa was prepared by the neutralization of 2-acrylamido-2-methylpropanesulfonic acid (>99%, Sigma) with 1*M* sodium hydroxide (Merck). VP (99%, Sigma) was distilled under reduced pressure. The AAm (>98%, Fluka), potassium persulfate (KPS; >99%, Sigma), MBA (>99%, Sigma), formaldehyde (37%, Merck), trisodium citrate dihydrate (citrate, >99%, Merck), and $AgNO_3$ (>99%, Merck) were used as received. Phosphate-buffered solution at pH 7.4 and 3-(4,5-dimethylthiazol-2-yl)−2,5-diphenyltetrazolium bromide (MTT) were purchased from Sigma and were used as received. Ultrapure (UP) water obtained from a Milli-Q water purification system was used in the experiments.

Cell Cultures

Primary cultures of human embryonic fibroblasts were provided by the National Center of Microbiology of the Institute of Health Carlos III (Madrid, Spain). The cells were maintained at 37°C in a humid atmosphere of 5% CO_2 in 25-mL culture flasks (Sarstedt). The culture medium used (complete medium) was Eagle's minimal essential medium (MEM) modified with 15 mM 4-(2-Hydroxyethyl)piperazine-1-ethanesulfonic acid (HEPES; Sigma) and supplemented with 10% fetal bovine serum (FBS; Gibco), 200 m*M* L-glutamine, 100 U/mL penicillin, and 100 μg/mL streptomycin (Sigma). The culture medium was changed at selected time intervals with care to disturb the culture conditions as little as possible.

Preparation of the Hydrogel–AgNPs Composites

The hydrogels were obtained by radical copolymerization in aqueous media of the monomers AAm/AMPSNa and VP/AMPSNa in a 1:1 molar ratio. 3 and 6 mol % of MBA were used for each copolymer system, and the total monomer concentration in the initial solution was 15 wt %. In all cases, the reagent mixture (contained in 40-mL Teflon tubes) was deoxygenated by the bubbling of pure nitrogen for 10 min, and then, the reaction was induced thermally at 60°C with 1 mol % KPS as free-radical initiator (without stirring). By 24 h later, the products were soaked in UP water for 2 days to remove residual solute and dried at 60°C. The yield of the copolymers (hydrogels) was determined gravimetrically. Then, 3 g from each hydrogel was immersed separately in 500 mL of a silver colloid previously prepared by the microwave oven heating of an aqueous solution (1000 mL) of 1 m*M* $AgNO_3$, 1 m*M* citrate, and 5 m*M* formaldehyde (24 on–off heating cycles of 20–20 s). After 24 h of immersion in the silver colloid at 25°C, the hydrogels were removed from the colloid, dried at 60°C, milled, and sieved through a 100-μm sieve.

Characterization of the Hydrogels, Hydrogel–AgNPs Composites, and Silver Colloid

The IR spectra of the hydrogels and composites were obtained on a Spectrum One spectrometer (PerkinElmer) with the attenuated total reflectance (ATR) Fourier transform infrared (FTIR) spectroscopy method. The spectra were recorded with 32 scans and a resolution of 4 cm^{-1}.

The scanning electron microscopy (SEM) images of the dried composites were acquired with a Hitachi model SU-8000

microscope operating at high vacuum. The dry samples were not coated with conductive materials, and they were analyzed at low voltage (1.0 kV). The energy-dispersive X-ray spectra (EDS) were obtained with a Bruker QUANTAX 200 spectrometer coupled to the SEM microscope.

The silver colloid used to prepare the composites was analyzed with a Lambda 35 ultraviolet–visible spectrophotometer (PerkinElmer) in the range from 200 to 800 nm. The particle size distribution and ζ potential of the colloid were obtained with a Zetasizer Nano ZS instrument (Malvern Instruments, Ltd.).

Quantification of the Total Silver Released from the Hydrogel–AgNPs Composites

Each of the composites (10 mg) was independently immersed in 20 mL of UP water in a sealed container at 25°C with constant agitation. After 96 h, the insoluble material was separated from the aqueous medium by filtration with a nylon mesh with 80-μm pores; the filtrates were subjected to acid digestion with 5 mL of concentrated nitric acid (65 wt %) and gentle heating to obtain a final volume of 10 mL. A series of standard solutions of ionic silver were also prepared with the same acid digestion conditions mentioned previously. All of the samples were diluted with UP water to a final volume of 50 mL and analyzed by atomic absorption spectroscopy to determine the concentration of silver in each of the samples. In this experiment, a hollow silver cathode lamp and an air–acetylene flame with a wavelength of 328.1 nm were used.

Antibacterial Activity Assay

A modified version of the hole–plate diffusion method was used to assess the antibacterial activity of the four composites,[17] four hydrogels (without nanosilver), and aqueous solutions of silver nitrate ($AgNO_3$) with silver concentrations of 108 and 5720 ppm, which were used as positive controls. The bacteria used were *E. coli* (ATCC 25922) and *S. aureus* (ATCC 6538P). The respective bacterial suspensions (100 μL) in trypticase soy broth prepared with cell densities of 4.5×10^7 cfu/mL for *E. coli* and 1.8×10^7 cfu/mL for *S. aureus* were homogeneously spread on plates of trypticase soy agar (TSA). Four equidistant wells with 9-mm diameters were made on the agar surface 20 mm from the edge of the agar plate, and 2.5 mg of each solid sample (dry powder sieved in a 100-μm pore size mesh) and 100 μL of each $AgNO_3$ solution was placed in separate wells. Then, 150 μL of water was added to the wells containing solid samples. The plate was kept at 4°C for 1.5 h to allow diffusion of the silver present in the samples. Then, the plates were incubated at 37°C for 18 h. Finally, the zones of inhibition (ZIs) were calculated by subtraction of the diameter of each well (9 mm) from its respective outer circular area (generated by the diffusion of the sample components). Agar plates with and without inoculum were also included as controls. The samples were tested in triplicate, and a one-way analysis of variance (ANOVA) was used to compare the mean ZIs produced. To determine the difference between the mean ZIs of different treatments, the least significant difference (LSD) test was used with a statistical significance of 0.05.

Cytotoxicity Assay

The potential cytotoxic effect of the composites and hydrogels in human embryonic fibroblast cultures was evaluated with an indirect MTT assay, which was repeated three times for each sample. Initially, 5 mg of each solid sample (composite and hydrogels) and a disc TMX (Thermanox Polystyrene, Lab-Clinics), which was used as negative control, were added to separate tubes containing 5 mL of FBS-free complete medium and were stirred for 1 day at 37°C. Then, the medium in contact with the samples, or eluent, was removed and stored at −20°C until further use. Eluents were also obtained from samples dipped in complete medium without FBS for 2 and 14 days. Subsequently, 100 μL of human fibroblast culture at a density of 8×10^4 cells/mL was added to each well of a 96-well culture plate. After culture incubation at 37°C in humidified air with 5% CO_2 for 24 h, the medium in each plate well was replaced by 100 μL of the respective eluents previously obtained (eight treatments) and 100 μL of a 20 m*M* hydrogen peroxide solution in MEM, which was used as positive control. After a 24-h incubation in the same conditions as used previously, the eluents and positive control medium were replaced with 100 μL of a solution of 0.5 mg/mL MTT in phosphate-buffered solution, and the cells were maintained at 37°C for an additional 4 h. Afterward, the MTT solution was removed, and 100 μL of dimethyl sulfoxide was added to each well to dissolve the blue crystals that formed. The plates were shaken for 5 min, and the absorbance was measured at 570 nm on a Biotek ELX808IU plate reader. The absorbance values recorded were used in the following equation to calculate the percentage cell viability (%VC) of each replica with respect to the TMX negative control:

$$\%VC = \frac{DO_M}{DO_C} \times 100$$

where DO_M and DO_C are the optical density measurements of the sample and the negative control, respectively. A one-way ANOVA was performed to compare the mean viability percentages generated by the composites, hydrogels, and negative control.

The composites or hydrogels were considered cytotoxic when they gave viability percentage values below 70%. To determine the difference between the mean percentages of viability of different treatments, we used the LSD test. When the p value was lower than 0.05, the differences among the treatments were considered significant.

Simultaneously, as a second positive control, the same procedure described previously was applied to 11 ionic silver solutions in MEM, which were prepared by twofold serial dilution from a concentration of 572 ppm.

RESULTS AND DISCUSSION

Hydrogels, Hydrogel–AgNPs Composites, and Silver Colloid

The hydrogels synthesized showed a high swelling capacity in aqueous media, which was observed when they were immersed in (1) UP water during the extraction of the reaction residues and (2) the silver colloid during preparation of the respective hydrogel–AgNP composites. To facilitate the identification of the four hydrogels, the following sample numbers were assigned: 7, 11, 15, and 22. The reaction yields for the four synthesized hydrogels and the milliliters of absorbed colloid per gram of dried hydrogel (xerogel) are recorded in Table I.

Table I. Reaction Yields Obtained in the Synthesis of the Hydrogels and Volumes of Colloid Absorbed per Gram of Xerogel

Sample	Monomer feed composition	Yield (%)	Colloid/dry sample (mL/g)
7	VP/AMPSNa (1:1), 3 mol % MBA	45	115
11	VP/AMPSNa (1:1), 6 mol % MBA	68	40
15	AAm/AMPSNa (1:1), 3 mol % MBA	97	40
22	AAm/AMPSNa (1:1), 6 mol % MBA	98	20

The ultraviolet–visible spectrum of the colloid obtained presented only one band with a maximum absorption at 434 nm, which corresponds to the surface plasmon resonance band of the colloidal silver.[18] The analysis of the colloid by dynamic light scattering system on the Nano Zetasizer equipment showed a bimodal particle size distribution with a meaningful amplitude (see Figure 1), which was consistent with the recorded polydispersity index of 0.596.[19] This bimodal distribution suggested the existence of two populations of particles with very different sizes in the colloid.[20] The particle diameter range and the mean value were 1.5–5.6 and 3.1 ± 0.4 nm, respectively, for the number 1 population and 14–164 and 50.7 ± 0.8 nm for the number 2 population. The ζ potential measured with the Nano Zetasizer equipment was -47.2 ± 1.3 mV; this indicated a high stability of the nanoparticles and the possible coating of its surface with citrate anions that functioned as stabilizer agents.[21] The colloid pH was 6.5.

A comparative analysis of the ATR–FTIR spectra between the composites and their respective original hydrogels is shown in Figure 2. The only difference observed was the higher signal intensity corresponding to the N—H stretching (ν) in the composite (between 3439 and 3220 cm^{-1}); this suggested a possible interaction between the AgNPs and the amino groups of the copolymer matrix.[22]

The ATR–FTIR spectra of all of the samples indicated the presence of the characteristic functional groups of the expected copolymers (see Figures 2 and 3) and the absence of vinyl signals (C=C stretching to 1630–1610 cm^{-1}).[23] The most characteristic bands of both copolymer systems were located in the following wave-number ranges: 3439–3220 cm^{-1} (N—H stretching of amine groups), 2980–2936 cm^{-1} (CH_2 symmetric and unsymmetric stretching), 1655–1650 cm^{-1} (C=O stretching of amides), 1544–1543 cm^{-1} (N—H bending of amine groups), 1183–1182 cm^{-1} (O=S=O asymmetric stretchings), and 1040 cm^{-1} (O=S=O symmetric stretchings). This result was evidence of the copolymerization of the monomers and the purity of the obtained product. Similar results were obtained for the other composites and hydrogels.

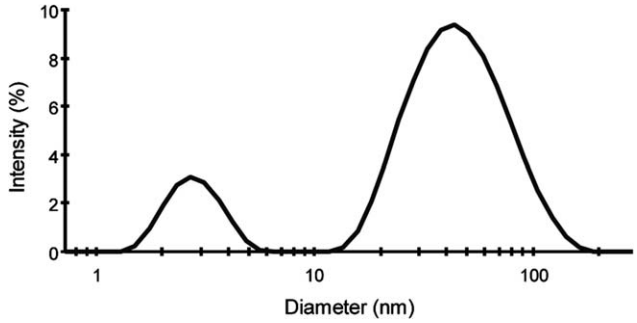

Figure 1. Size distribution measured by the scattered light intensity of the AgNPs in the colloid used to prepare the composites.

The SEM images of the composites confirmed the presence of nanoparticles with diameters greater than 6 nm on their outer surface (see Figure 4). The EDS spectra of the outer surface and cross sections of each composite were almost identical and showed a signal at about 3 keV, which corresponded to the incorporated silver (see Figure 5). It is likely that this signal was generated by both the produced AgNPs and the silver ions that did not react during the preparation of the silver colloid used to prepare the composites.

Antibacterial Activity of the Hydrogel–AgNPs Composites

The results shown in Table II and Figures 6–8 clearly indicate the presence of antibacterial activity in the composites because the ZIs of bacterial growth were generated on the surface of the TSA culture plates. On the other hand, the hydrogels did not inhibit bacterial growth (samples 7, 11, 15, and 22 in Table II); this indicated that the antibacterial effect found in the composites could be attributed to the silver (AgNPs and residual silver ions).

For hydrogels containing AAm (15 and 22) and those containing VP (7 and 11), the hydrogels with a lower percentage of crosslinker (3 mol % MBA) absorbed greater silver colloid volumes (see Table I) during the preparation of the respective composites. As a result, the composites from these hydrogels incorporated a higher amount of silver (previously confirmed by thermogravimetric analysis)[24] and released a higher amount of silver when immersed in water (see Table II). This was more evident for those composites containing VP (5 and 9) than for those containing AAm (13 and 18) because the first group of composites, the one with lower degree of crosslinking, showed a silver released percentage five times larger than that with a higher degree of crosslinking; this explains the big difference in the means ZI diameters generated by them (see Table II).

However, in the composites containing AAm, the silver released percentage was 0.2 times larger in favor of that with lower

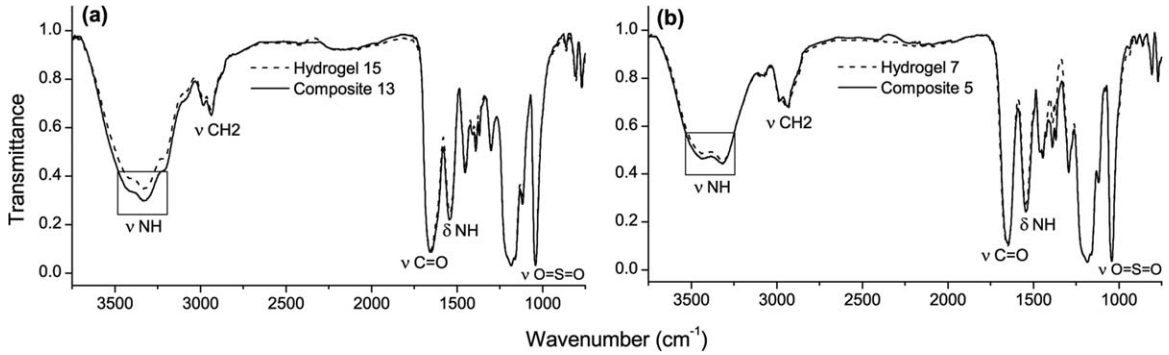

Figure 2. Comparison of the ATR–FTIR spectra for (a) composite 13 and hydrogel 15 and (b) composite 5 and hydrogel 7. The amino group stretching frequencies (shown in the squares) were more intense in the spectra of the composites.

degree of crosslinking, which explains the very similar mean ZI diameters.

The ZI diameters (in millimeters) obtained in the assay with *E. coli* were transformed by the expression $\log(x - 0.8)$ to fit them to a normal distribution (χ^2 goodness-of-fit test, $p = 0.253551$, and Shapiro–Wilks test, $p = 0.329549$) and the assumption of homogeneity of variance was confirmed for these data (Cochran test, $p = 0.216297$, and Bartlett test, $p = 0.0802876$). The ANOVA results indicate that there were significant differences between at least two of the mean ZI diameters generated by the treatments (composites and control solutions of Ag^+, $p = 0.000$).

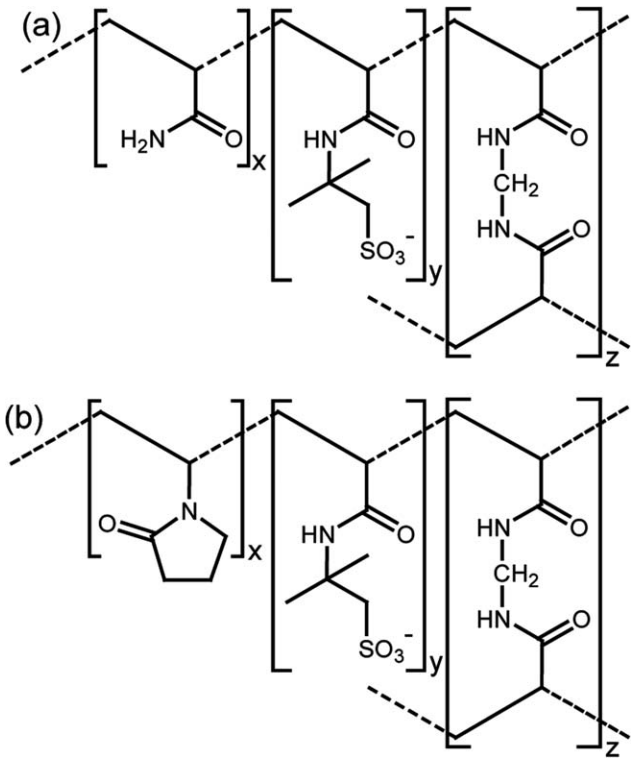

Figure 3. Molecular structure of the hydrogels and hydrogel–AgNPs composites coming from (a) poly(AAm-*co*-AMPSNa) and (b) poly(VP-*co*-AMPSNa).

The differences among the means were examined with the pairwise comparisons method or Fischer's LSD method.

The most significant differences were found among the mean ZI diameter of composite 5 and those generated by the other three composites (9, 13, and 18); its mean ZI diameter was between 37 and 83% greater than the other three; this made it the composite with the highest antibacterial capacity. Furthermore, the mean ZI diameter of composite 5 was 33% lower than that generated by silver nitrate with a concentration of 108 ppm Ag (positive control). The differences between the mean ZI diameters of composites 9, 13, and 18 did not exceed 0.3 mm when they were compared pairwise, and they could, therefore, be considered to have nearly equivalent antibacterial efficacies.

In the assay performed with *S. aureus,* the ZI diameters (in millimeters) obtained were also adjusted to a normal distribution (χ^2 goodness-of-fit test, $p = 0.178278$, and Shapiro–Wilks test, $p = 0.195171$) after their transformation with the expression $\log(x - 0.85) + (1/x)$. For these data, the assumption of homogeneity of variance also met the criteria (Cochran test, $p = 0.158186$, and Bartlett test, $p = 0.479333$), and therefore, the one-way ANOVA test for their analysis could be used. The one-way ANOVA analysis revealed significant differences between at least two of the mean ZI diameters generated by the treatments ($p = 0.000$).

The LSD test was applied to the mean ZI diameters, and the results show that the largest significant differences occurred between composite 5 and composites 9, 13, and 18; the mean ZI diameter of composite 5 was between 75 and 100% greater than those of the other composites. The mean ZI diameter of composite 5 was equal to that generated by silver nitrate with a concentration of 108-ppm Ag (positive control). There were no significant differences between the mean ZI diameters of composites 9, 13, and 18.

Furthermore, the lower colloid volume absorbed by hydrogels 15 and 22 with respect to hydrogels 7 and 11 (see Table I) was likely because of the presence of the lateral amide groups of the AAm, which increased the number of intercatenary and intracatenary hydrogen bonds into their crosslinked polymeric matrix (the interactions between lateral amide groups could be of the following types: AAm–AAm, AAm–AMPSNa, and AMPSNa–

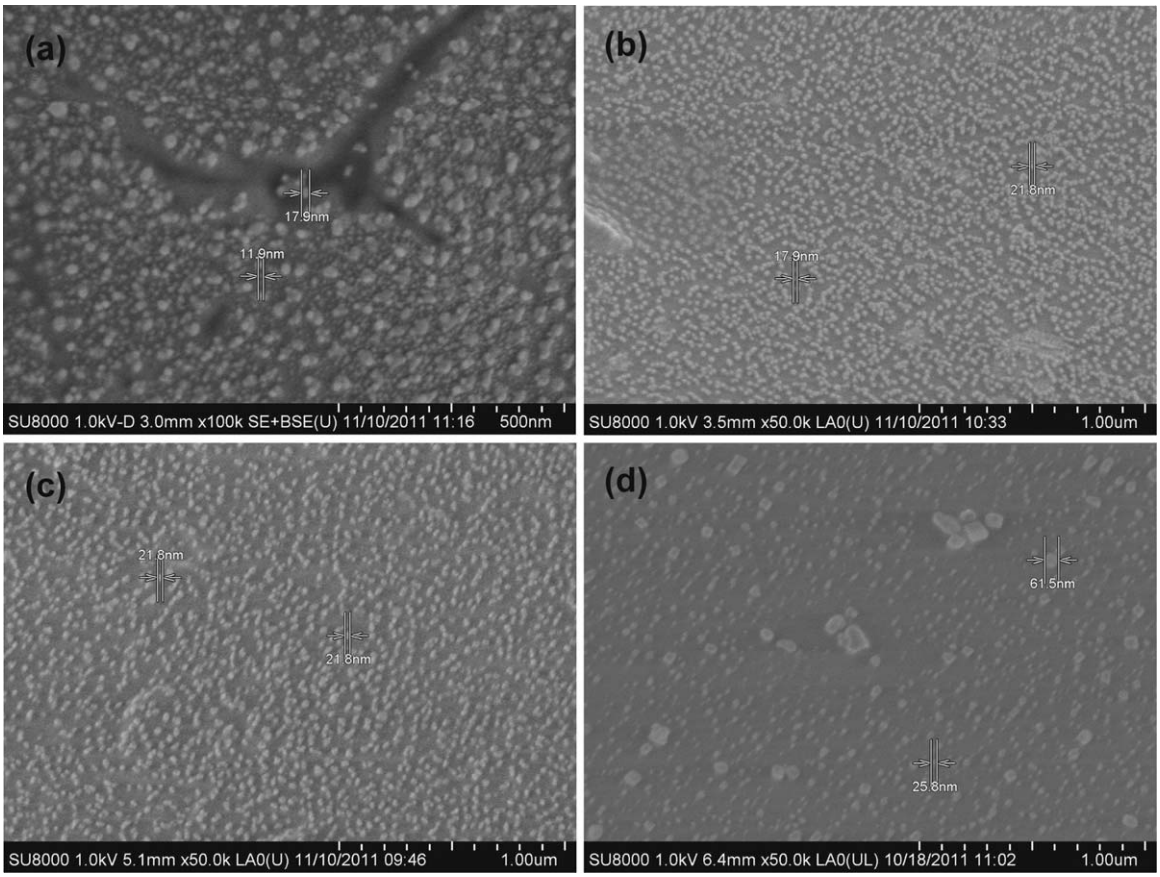

Figure 4. Scanning electron micrographs of the outer surfaces of the hydrogel–AgNPs composites: (a) 5, (b) 9, (c) 13, and (d) 18.

AMPSNa). This conferred greater resistance to relaxation of the polymer chains in the presence of aqueous media and, therefore, decreased the absorption of the medium components.[25]

Such hydrogen bonds were also present in hydrogels 7 and 11 but in a smaller number because the nitrogen atom of the lateral group of VP lacked the hydrogen, and only the lateral group of AMPSNa could form such bonds. According to the IR spectra of the composites prepared with the aforementioned hydrogels, the AgNPs (and silver ions) interacted with the amino groups (NH) of the polymer, but in the interior of the polymeric systems based on AAm (hydrogels 15 and 22 and composites 13 and 18), there were fewer available amino groups to interact with the silver because of the formation of hydrogen bonds between the groups. Hence, the superficial amino groups would form the majority of the existing hydrogen bonds with silver. Consequently, it was likely that the AgNPs were mostly located on the surface and outermost sublayers (less depth) for composites 13 and 18, whereas in composites 5 and 9, they were distributed in a homogeneous way.

According to the previous analysis, the amount of silver that could be incorporated into the hydrogels based on AAm depended largely on the surface area, and although it also depended on the crosslinking density, the crosslinking density was not a determining factor in the process. This conclusion was confirmed by the observation that composite 13, which had a lower degree of crosslinking and twice the colloid absorbed volume of composite 18 (see Table I), showed a value of silver release percentage similar to that of composite 18 (0.67 and 0.56%, respectively; see Table II). Keep in mind that all of the samples exhibited similar particle sizes because they were sieved with a 100-μm pore diameter sieve. The difference in volume of the colloid absorbed for these hydrogels was likely due mostly to the absorption of the water, in which the AgNPs were suspended.

Unlike in the previous case, the hydrogels that were based on VP had a smaller number of intercatenary and intracatenary hydrogen bonds; this increased the relaxation of the polymer chains and thus allowed a larger amount of AgNPs and water to be incorporated into the hydrogel by diffusion from the colloid. In this case, the amount of incorporated silver was limited by the increase in the degree of crosslinking of the hydrogel and thus by the hydrogel swelling. This was suggested from the percentages of total silver released by composites 5 and 9 (2.42% vs 0.46%, see Table II), whose concentrations of crosslinking reagent were 3 and 6 mol %, respectively.

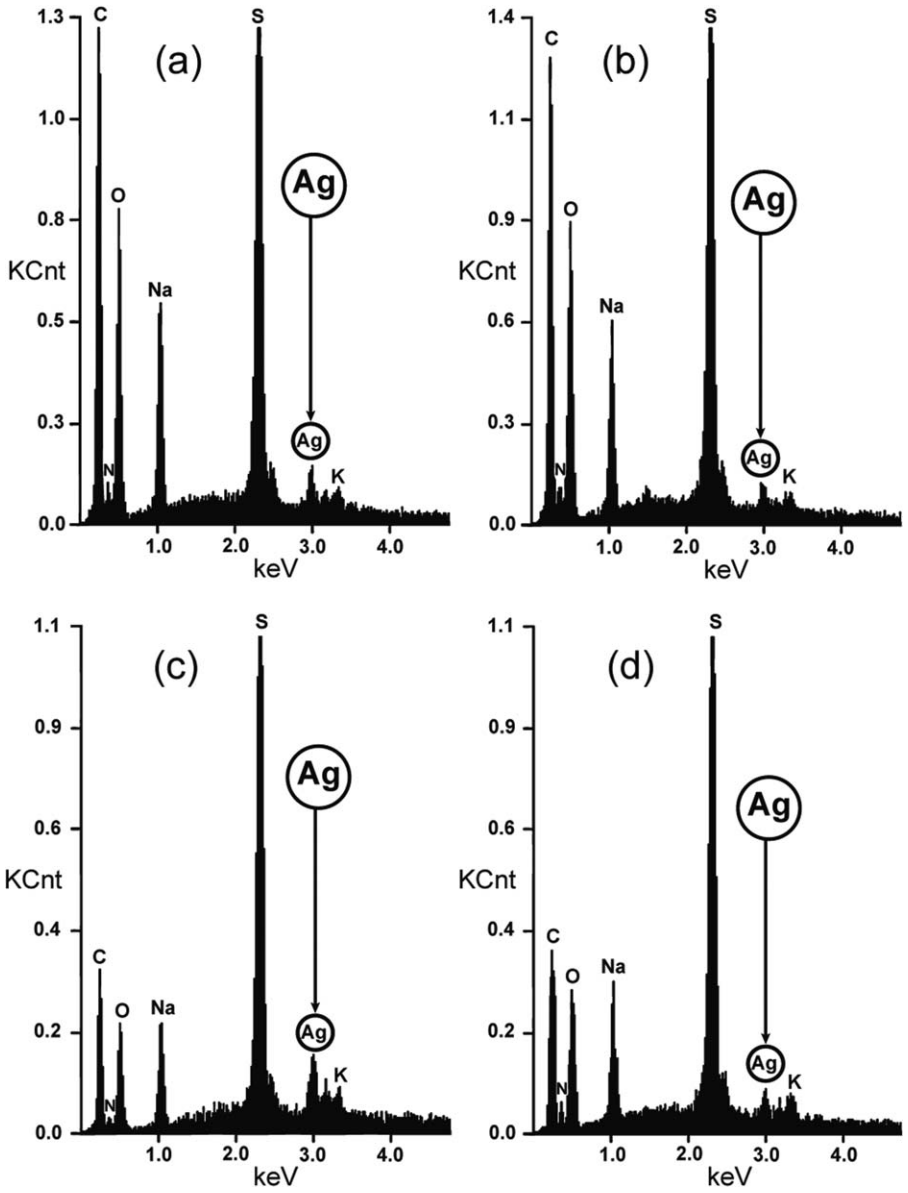

Figure 5. Cross-sectional EDS spectra of the hydrogel–AgNPs composites: (a) 5, (b) 9, (c) 13, and (d) 18. The horizontal axis is energy in kilo electron volts (KeV) and the vertical axis is intensity in kilo counts (KCnt).

Cytotoxicity of the Hydrogel–AgNPs Composites

The results of the cytotoxicity assay (see Figures 9 and 10) and the antibacterial activity assay (see Figure 6) of the composites confirmed the previous hypothesis regarding the AgNPs distribution in the composites and its relationship with the percentage of silver released (in aqueous medium).

Note that the cell viability of composites 13 and 18 (see Figure 10) was slightly less than that of composites 5 and 9 (see Figure 9). This was likely because the majority of the AgNPs were distributed on their surface (as mentioned previously); this led to a rapid and massive release of nanoparticles (a process known as *burst release*), which increased the cytotoxicity on the culture of fibroblasts.[26]

In contrast, the cell viability of composites 5 and 9 was closer to that observed for the negative control (TMX); this indicated a slower and more steady release of AgNPs (and all of the other potentially released components) compared with composites 13 and 18 because of their more uniform distribution in the polymer matrix.[26] Therefore, they did not cause substantial damage to the fibroblast cellular integrity.

Moreover, the cell viability values for composites 5 and 9 were slightly greater than those generated by their respective hydrogels (7 and 11; see Figure 9). This observation could be explained by a combination of two possible causes: (1) the presence of residual amounts of monomers in the hydrogel (which

Table II. ZI Produced by Samples on the Surfaces of TSA Plates Containing *E. coli* and *S. aureus* Bacteria and Weight Percentages of Total Silver Released from the Composites after Immersion in UP Water for 4 Days

Sample	Monomer feed composition	Ag released in water (%)	ZI ± standard deviation (mm)	
			E. coli	*S. aureus*
5	VP/AMPSNa (1:1), 3 mol % MBA	2.42	2.2 ± 0.1	2.8 ± 0.2
7	VP/AMPSNa (1:1), 3 mol % MBA	—	0	0
9	VP/AMPSNa (1:1), 6 mol % MBA	0.46	1.2 ± 0.2	1.4 ± 0.2
11	VP/AMPSNa (1:1), 6 mol % MBA	—	0	0
13	AAm/AMPSNa (1:1), 3 mol % MBA	0.67	1.3 ± 0.2	1.6 ± 0.1
15	AAm/AMPSNa (1:1), 3 mol % MBA	—	0	0
18	AAm/AMPSNa (1:1), 6 mol % MBA	0.56	1.6 ± 0.2	1.6 ± 0.2
22	AAm/AMPSNa (1:1), 6 mol % MBA	—	0	0
108 ppm Ag^+	NA	NA	3.3 ± 0.5	2.8 ± 0.3
5720 ppm Ag^+	NA	NA	3.5 ± 0.2	4.1 ± 0.2

NA, not applicable.

was not detected by ATR–FTIR spectroscopy) and (2) the presence of citrate anions in the composite, which promoted fibroblast growth and exhibited antibacterial activity according to histopathological studies in patients with wounds.[27] On the contrary, in the case of composites 13 and 18, the beneficial effect of the released citrate was most likely inhibited by the burst release phenomenon of silver that was mentioned previously. In Figure 10, note that the values of cell viability for hydrogels 15 and 22 were very similar to those recorded for the negative control (TMX); this demonstrated that the hydrogels did not release cytotoxic components.

The final concentrations of total silver ($Ag^0 + Ag^+ = Ag$) in the fibroblast cultures were estimated assuming that the percentages of silver released from the composites into the culture medium (MEM) were equal to those obtained in UP water (see Table II). The estimated silver concentrations in MEM corresponding to composites 5, 9, 13, and 18, were 24.2, 4.6, 6.7, and 5.6 ppm, respectively, and were compared the cell viability values generated by these treatments against those generated by the serial dilutions $AgNO_3$ prepared as positive control (see Figure 11).

The results of this comparison indicate that the extracts taken on different days (days 1, 2, and 14) for all of the composites produced viable cell populations between five and eight times larger than those generated by dilutions of silver nitrate with similar silver concentrations. This means that in the silver concentration range evaluated, the aqueous mixtures of the AgNPs and the silver ions with the same concentrations of silver as the silver nitrate solutions used as positive controls were less toxic to fibroblasts.

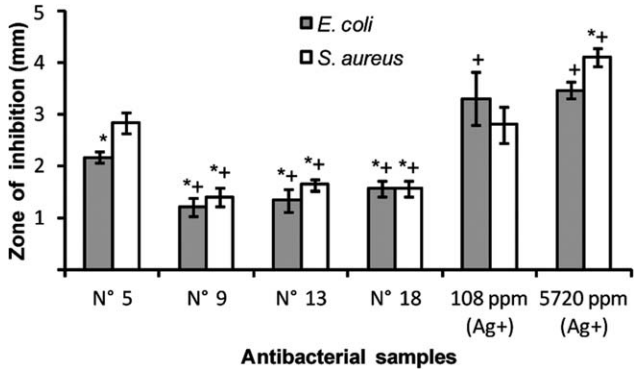

Figure 6. ZI (mm) produced by the hydrogel–AgNPs composites and positive controls (Ag^+) on TSA plates seeded with *E. coli* (gray bars) and *S. aureus* (white bars). The data represent the means and standard deviations of the mean ($n = 3$) and significant differences (revealed by ANOVA tests) with respect to 108-ppm Ag^+ ($^*p < 0.05$) and composite 5 ($^+p < 0.05$).

CONCLUSIONS

The following conclusions were drawn: (1) it was possible to incorporate AgNPs into the crosslinked hydrogels poly(VP-*co*-AMPSNa) and poly(AAm-*co*-AMPSNa) by immersion of the hydrogel in colloid silver; (2) among the four composites prepared in this study, composite 5, which came from the hydrogel poly(VP-*co*-AMPSNa) and was synthesized with a 1:1 feed molar ratio of monomers and 3 mol % MBA, exhibited the highest antibacterial activity against *E. coli* and *S. aureus,* as measured by the hole–plate diffusion method; and (3) composite 5 was also the least cytotoxic to human fibroblasts, as measured by an indirect MTT assay, generating percentages of cell viability greater than 80% (% TMX). These results are highly promising for the possible use of composite 5 as a dressing for the treatment of deep and exudative wounds.

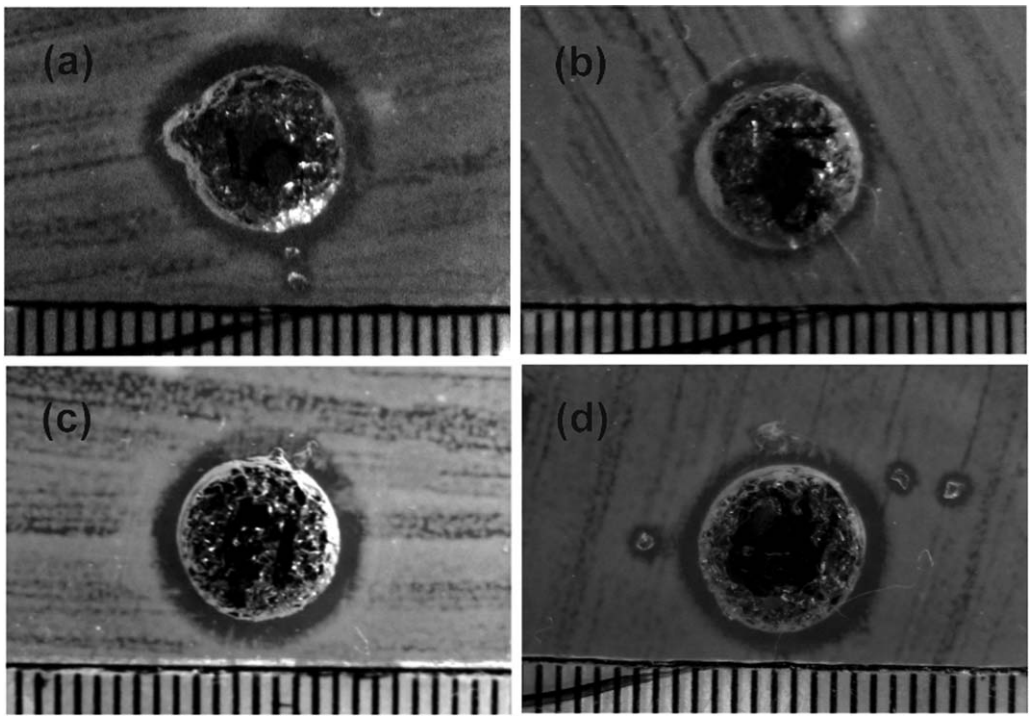

Figure 7. Results of the hole–plate diffusion assays of the hydrogel–AgNPs composites against *E. coli* (ATCC 25922) after 18 h of incubation at 37°C: (a) 5, (b) 9, (c) 13, and (d) 18.

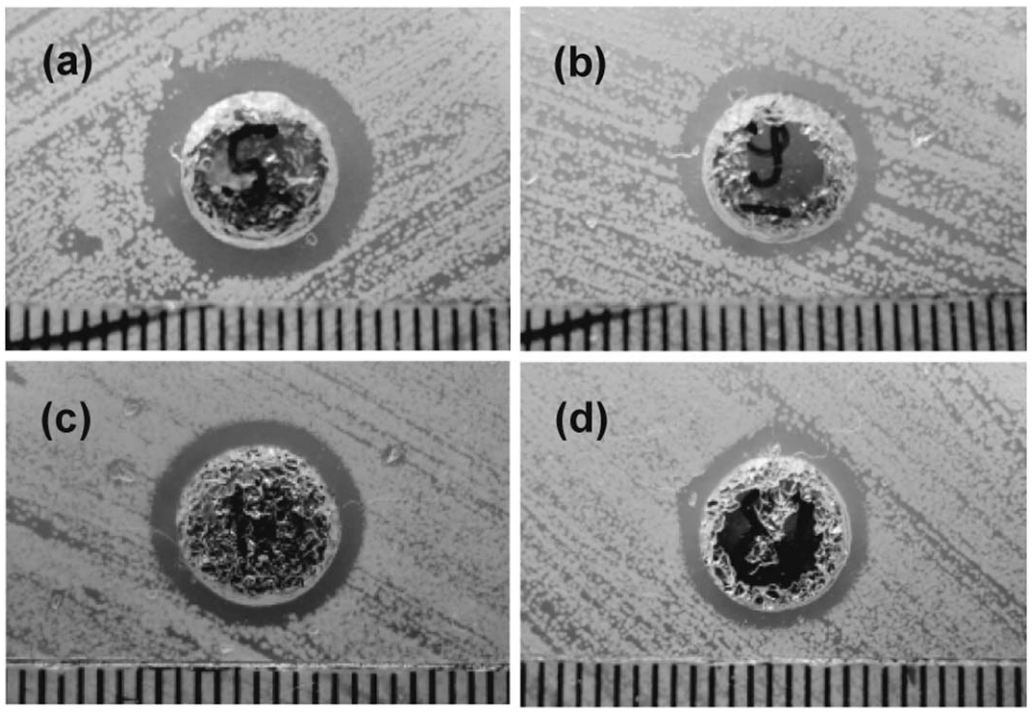

Figure 8. Results of the hole–plate diffusion assays of the hydrogel–AgNPs composites against *S. aureus* (ATCC 6538P) after 18 h of incubation at 37°C: (a) 5, (b) 9, (c) 13, and (d) 18.

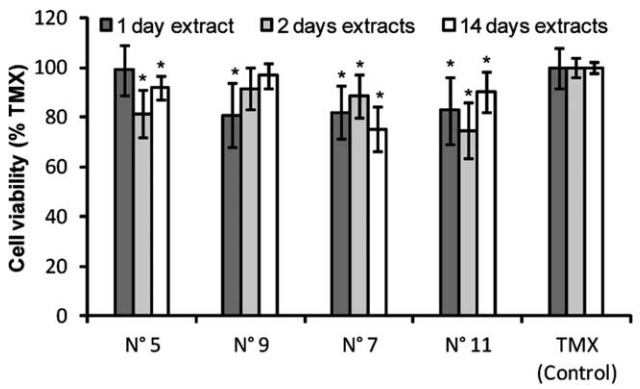

Figure 9. Percentage cell viability with respect to TMX generated by extracts (in MEM) of the poly(VP-*co*-AMPSNa)-type composites (5 and 9) and hydrogels (7 and 11) on human embryonic fibroblasts. Three extracts (eluents) per sample were evaluated and corresponded to samples obtained after 1, 2, and 14 days of extraction. The data represent the means and standard deviations of the mean ($n = 8$) and significant differences (revealed by ANOVA tests) with respect to TMX ($^*p < 0.05$).

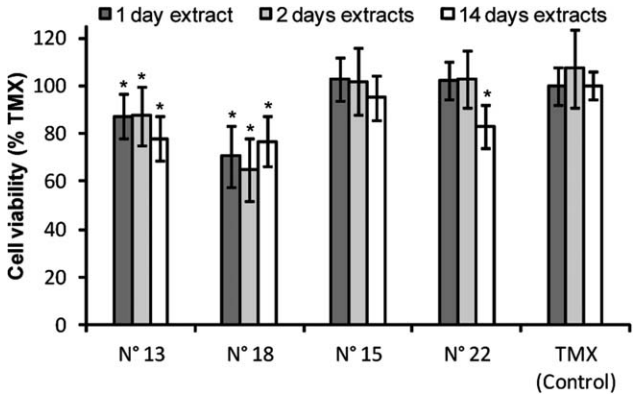

Figure 10. Percentage cell viability with respect to TMX generated by extracts (in MEM) of the poly(AAm-*co*-AMPSNa)-type composites (13 and 18) and hydrogels (15 and 22) on human embryonic fibroblasts. Three extracts (eluents) per sample were evaluated and corresponded to samples obtained after 1, 2, and 14 days of extraction. The data represent the means and standard deviations of the mean ($n = 8$) and significant differences (revealed by ANOVA tests) with respect to TMX ($^*p < 0.05$).

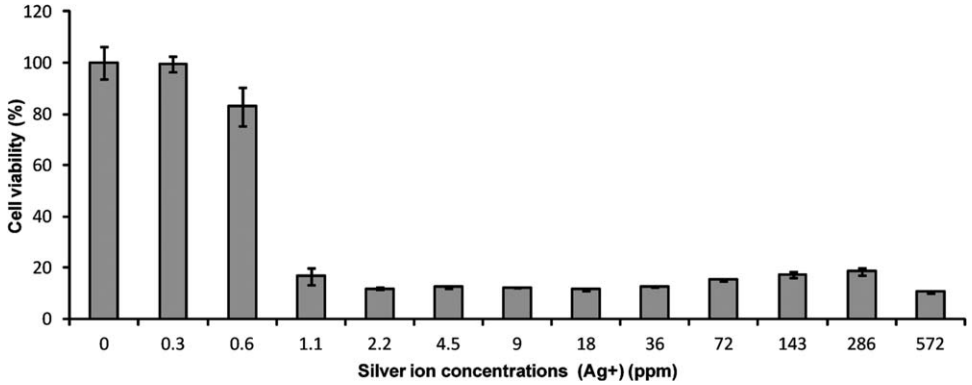

Figure 11. Percentage cell viability generated by $AgNO_3$ serial dilutions (in MEM) on human embryonic fibroblasts. The $AgNO_3$ solution concentrations are expressed in terms of silver ions (Ag^+). The data represent the means and standard deviations of the mean ($n = 3$).

ACKNOWLEDGMENTS

The authors thank Fondo Nacional de Desarrollo Científico y Tecnológico (contract grant number 1110079) and Programa de Investigación Asociativa (contract grant Anillo ACT-130). One of the authors (H.V.) thanks Comisión Nacional de Investigación Científica y Tecnológica de Chile for a scholarship awarded for doctoral studies.

REFERENCES

1. Branski, L. K.; Al-Mousawi, A.; Rivero, H.; Jeschke, M. G.; Sanford, A. P.; Herndon, D. N. *Surg. Infect. (Larchmt.)* **2009**, *10*, 389.
2. Morones, J. R.; Elechiguerra, J. L.; Camacho, A.; Holt, K.; Kouri, J. B.; Tapia Ramírez, J.; Yacamán, M. *J. Nanotechnol.* **2005**, *16*, 2346.
3. Castellano, J. J.; Shafii, S. M.; Ko, F.; Donate, G.; Wright, T. E.; Mannari, R. J.; Payne, W. G.; Smith, D. J.; Robson, M. C. *Int. Wound J.* **2007**, *4*, 114.
4. Dallas, P.; Sharma, V. K.; Zboril, R. *Adv. Colloid Interface Sci.* **2011**, *166*, 119.
5. Alt, V.; Bechert, T.; Steinrücke, P.; Wagener, M.; Seidel, P.; Dingeldein, E.; Domann, E.; Schnettler, R. *Biomaterials* **2004**, *25*, 4383.
6. El-Badawy, A.; Feldhake, D.; Venkatapathy, R. State of the Science Literature Review: Everything Nanosilver and More; U.S. Environmental Protection Agency: Washington, DC, **2010**; p 67.
7. Thomas, V.; Murali Mohan, Y.; Sreedhar, B.; Bajpai, S. K. *J. Appl. Polym. Sci.* **2009**, *111*, 934.
8. Rigo, C.; Ferroni, L.; Tocco, I.; Roman, M.; Munivrana, I.; Gardin, C.; Cairns, W. R. L.; Vindigni, V.; Azzena, B.; Barbante, C.; Zavan, B. *Int. J. Mol. Sci.* **2013**, *14*, 4817.
9. Nalampang, K.; Suebsanit, N.; Witthayaprapakorn, C.; Molloy, R. *Chiang Mai J. Sci.* **2007**, *34*, 183.
10. Üzüm, Ö. B.; Kundakci, S.; Karadag, E. *Polym. Bull.* **2006**, *57*, 703.

11. Parambil, A. M.; Puttaiahgowda, Y. M.; Shankarappa, P. *Turk. J. Chem.* **2012**, *36*, 397.
12. Rodríguez-Lorenzo, L. M.; García-Carrodeguas, R.; Rodríguez, M. A.; De Aza, S.; Jiménez, J.; López-Bravo, A.; Fernández, M.; San Román, J. *J. Biomed. Mater. Res. Part A.* **2009**, *88*, 53.
13. Gatica, N.; Fernández, N.; Opazo, A.; Radic, D. *J. Chil. Chem. Soc.* **2005**, *50*, 581.
14. Saraydin, D.; Koptagel, E.; Unver-Saraydin, S.; Karadag, E.; Guven, O. *J. Mater. Sci.* **2001**, *36*, 2473.
15. Bajpai, A. K.; Shukla, S. K.; Bhanu, S.; Kankane, S. *Prog. Polym. Sci.* **2008**, *33*, 1088.
16. Elvira, C.; Mano, J. F.; San Román, J.; Reis, R. L. *Biomaterials* **2002**, *23*, 1955.
17. Brantner, A.; Males, Z.; Pepeljnjak, S.; Antolic, A. *J. Ethnopharmacol.* **1996**, *52*, 119.
18. Ling, J.; Sang, Y.; Huang, C. Z. *J. Pharm. Biomed. Anal.* **2008**, *47*, 860.
19. Zetasizer Nano User Manual MAN0317; Malvern Instruments: Malvern, United Kingdom, **2009**; Issue 5.0, Chapter 15, p 15.1.
20. MacCuspie, R.; Rogers, K.; Patra, M.; Suo, Z.; Allen, A. J.; Martin, M. N.; Hackley, V. A. *J. Environ. Monit.* **2011**, *13*, 1212.
21. Henglein, A.; Giersig, M. *J. Phys. Chem. B.* **1999**, *103*, 9533.
22. Luo, Y. L.; Xu, F.; Chen, Y. S.; Jia, C. Y. *Polym. Bull.* **2010**, *65*, 181.
23. Pretsch, E.; Bühlmann, P.; Affolter, C.; Herrera, A.; Martínez, R. Determinación Estructural de Compuestos Orgánicos; Masson: Barcelona, **2002**; p 245.
24. Valle, H.; Rivas, B. L.; Aguilar, M. R.; San Román, J. *J. Appl. Polym. Sci.* **2013**, *129*, 537.
25. Shestakova, P.; Willem, R.; Vassileva, E. *Chem.–Eur. J.* **2011**, *17*, 14867.
26. Huang, X.; Brazel, C. S. *J. Controlled Release* **2001**, *73*, 121.
27. Nagoba, B. S.; Gandhi, R. C.; Wadher, B. J.; Potekar, R. M.; Kolhe, S. M. *J. Med. Microbiol.* **2008**, *57*, 681.